Shimming Strategies for the Neck and C-Spine: A Computational Study

K. M. Koch[1], and J. A. Stainsby[2]

[1]Applied Science Laboratory, GE Healthcare, Waukesha, WI, United States, [2]Applied Science Laboratory, GE Healthcare, Toronto, Ontario, Canada

Introduction: B_0 perturbations in the lower head and neck regions severely distort echo-planar images (EPI) and therefore impact diffusion-tensor imaging (DTI) of the c-spine. Fat suppression and spectroscopic techniques are also degraded by B_0 inhomogeneity in these regions. Here, a computational study is presented whereby the efficacies of different room-temperature shimming schemes are evaluated in the neck and c-spine region. Static first-order, static second order, dynamic first-order [1], and dynamic second-order shim [2] strategies are implemented on a computed B_0 distribution. Residual ΔB_0 distribution maps are presented, along with histogram and quantitative EPI distortion analysis.

Methods: A high-resolution ΔB_0 distribution in the c-spine region was computed for B_0 = 3 Tesla using an FFT-based first-order approximated solution to Maxwell's equations [3][4][5]. This method, which requires a 3D magnetic susceptibility distribution input, has been shown to accurately predict the anatomically induced ΔB_0 distribution in the human brain [5]. For the present study, the Visual Human® (NLM, Bethesda, MD) model was utilized, which provided a computational grid of 196x114x626 pixels over 58.8 cm x 34.2 cm x 187.8 cm. The full visual human model was binned into air, tissue and bone compartments, which were assigned respective magnetic susceptibilities of 0.3 ppm, -9.2 ppm, and -11.3 ppm [6]. The B_0 perturbations induced by this 3D magnetic susceptibility distribution were then computed using methods identical to those described in [5].

Thirty-one 3mm axial slices encompassing the c-spine region (9.3 cm coverage) were identified and selected from the whole-body ΔB_0 computation for shim analysis. An analysis ROI was selected by identifying all pixels in the selected slices of the visual human model that were not air, bone, or teeth. First-order global, second-order global, first order slice-specific, and second-order slice specific shim settings were optimized over this ROI. Slice-specific dynamic shim settings were calculated using degenerate shim analysis as reported in [2]. Global and slice-specific shim settings were found to be within typical shim coil constraints.

Histograms with 2 Hz bin widths were calculated for each shim setting and a frequency-centered non-shimmed map. Histogram widths were then quantified with central frequency offset ranges containing 75 percent of pixels in the ROI. The impact on EPI distortion was quantified by calculating the percentage of pixels in the ROI that had absolute offsets greater than 120 Hz. Pixels at offsets greater than this value will be displaced at least 2 pixel widths in the phase-encoded direction of an EPI image collected with 64x64 in plane pixels and a 250 kHz readout bandwidth (assuming infinitesimally short gradient ramps).

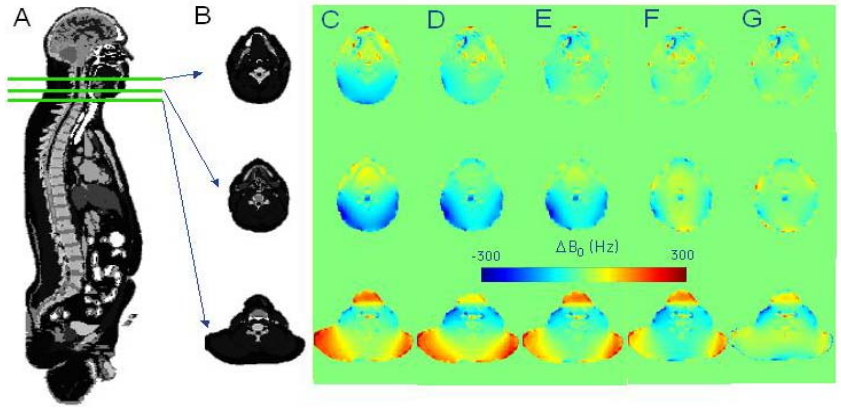

Figure 1. A) Sagittal view of input model showing axial slice locations, B) axial images of anatomic model, computed residual B_0 inhomogeneity maps after C) no shimming, D) 1st order global (static), E) 2nd order global, F) 1st order slice-specific (dynamic), and G) 2nd order slice-specific shim settings.

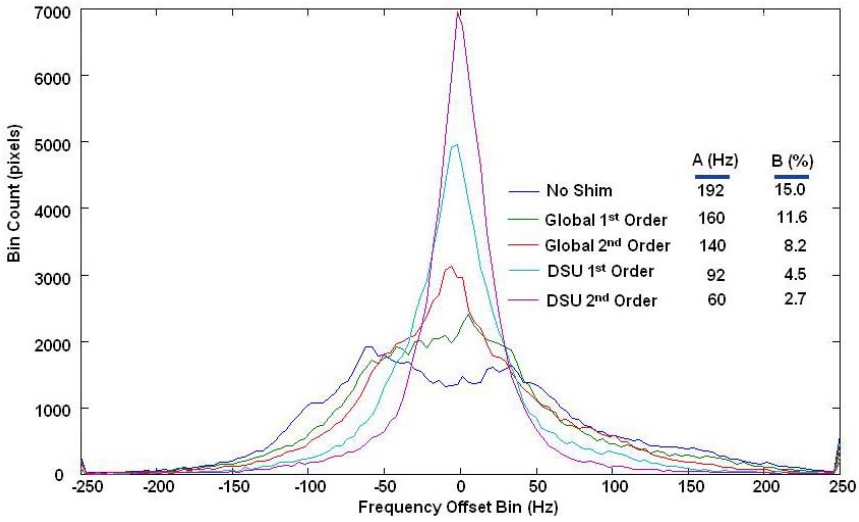

Figure 2. Frequency offset histograms computed over tissue-identified pixels in 31 3 mm axial slices in the c-spine region , A) histogram widths, and B) percentages of pixels displaced by at least 2 pixel widths in described EPI experiment for each shim setting.

Results and Discussion: The residual ΔB_0 maps in Figure 1 and the quantitative analysis provided in Figure 2 show the relatively limited capabilities of both 1st and 2nd order *static* shimming near the c-spine. Even after an optimized 0th through 2nd-order static global shim setting, enough residual inhomogeneity remains to severely compromise MR measurements. On the contrary, slice-specific *dynamic* shim settings were able to markedly improve the homogeneity even when using only 0th and 1st order shims. With this shim setting, less than 5% of MR-visible pixels in the model would be distorted by more than 2 pixels in the previously described EPI experiment. On most MR hardware platforms, rapid dynamic changes of 2nd order shims require significant hardware revisions and additions [2]. However, dynamic changes of 1st order shim settings can be implemented with greatly reduced (if any) hardware modifications. The results presented here suggest that such a shimming approach could significantly improve ΔB_0-sensitive MR measurements near the c-spine. Future work will implement this shimming scheme and explore its application-specific benefits (such as EPI-based DTI of the c-spine).

[1] A Blamire et al, MRM, **36**, (1996)
[2] KM Koch et al, JMR, **180** (2006)
[3] R. Salomir et al, Concepts in Magn. Reson B., **19B**, (2003)
[4] JP Marques, R. Bowtell, Concepts in Magn. Reson. B., **25B**, (2005)
[5] KM Koch et al, Phys. Med. Biol, **52**, (2006)
[6] JA Hopkins and FW Wehrli, MRM, **37**, (1997)